DESDE 2013
https://repository.uaeh.edu.mx/revistas/index.php/icbi/issue/archive
Pädi Boletín Científico de Ciencias Básicas e Ingenierías del ICBI
ISSN: 2007-6363

Publicación Semestral Pädi Vol. 12 No. Especial 4 (2024) 344–351

Active attitude control applications for rockets based on a reconfigurable reaction wheel array
Aplicaciones de control activo de actitud para cohetes basadas en un arreglo de ruedas de reacción reconfigurable

Victor M. Lechuga-Gerónimo [a,*], Enid Partida-Herrera [b]

[a] *Department of Automatic Control, Centro de Investigación y de Estudios Avanzados (CINVESTAV)-IPN, 07360, Ciudad de México, México.*
[b] *Departament of Control and Automation, ESIME-IPN, 07360, Ciudad de México, México.*

Abstract

Reaction wheels are extremely useful actuators for attitude (orientation) control of various aerospace bodies; for example, satellites, aircraft, airplanes, drones and rockets. Among their virtues are high durability, controllability, efficiency, cleanliness and performance. These properties are enhanced if the reaction wheels are arranged in groups of two or more actuators, known as arrays. However, one of the areas of opportunity for arrays is the loss of a degree of freedom when a reaction wheel fails; which could imply the failure of the mission for the aerospace object and lead it to the abrupt end of its life. Although this property called redundancy has been the subject of study in recent times, there is no solution that guarantees the continuity of the mission of the aerospace object under the scenario of fatal failure of one, or more, reaction wheels of an array. To solve the above problem, this work developed an engineering proposal based on the use of a mathematical model for a rocket that allows the reaction wheels of an array to be relocated within the body in a dynamic, independent and safe manner to increase the redundancy of the actuators, and therefore, ensure the continuity of the mission. The product of this research, a technical proposal, is based on the conventional and widely used type of control to modify the attitude of rockets, known as Thrust Vector Control (TVC), and is combined with reaction wheels instead of conventional electromechanical actuators.

Keywords: control, attitude, rocket, reaction wheel, tvc.

Resumen

Las ruedas de reacción son actuadores sumamente útiles para el control de actitud (orientación) de diversos cuerpos aeroespaciales; por ejemplo, satélites, aeronaves, aviones, drones y cohetes. Entre sus virtudes se encuentran la alta durabilidad, controlabilidad, eficiencia, limpieza y rendimiento. Estas propiedades se potencializan si las ruedas de reacción se hallan en grupos de dos o más actuadores, denominados como arreglos. Sin embargo, una de las áreas de oportunidad para los últimos es la pérdida de un grado de libertad cuando una de ellas entra, de manera irreversible, en modo de falla; lo que podría implicar el fracaso de la misión para el objeto aeroespacial y desplazarlo al abrupto fin de su vida útil. Si bien esta propiedad denominada como redundancia ha sido motivo de estudio en épocas recientes, no existe una solución tal que garantice la continuidad de la misión del objeto aeroespacial bajo el escenario de falla fatal para una, o más, ruedas de reacción de un arreglo. Con el fin de subsanar la problemática anterior, en este trabajo se realizó una propuesta de ingeniería basada en el uso de un modelo matemático para cohetes que permita reubicar las ruedas de reacción de un arreglo en su interior de una manera dinámica, independiente y segura, con el fin incrementar la redundancia de los actuadores, y con ello, asegurar la continuidad de la misión. La propuesta parte de la técnica convencional y ampliamente usada para modificar la actitud de los cohetes, denominada como Control de Vector de Empuje (TVC, por sus siglas en inglés), y que pretende emplear ruedas de reacción en lugar de los actuadores electromecánicos convencionales.

Palabras Clave: control, actitud, cohete, rueda de reacción, tvc.

*Autor para correspondencia: victor.lechuga@cinvestav.mx
Correo electrónico: victor.lechuga@cinvestav.mx (Víctor Manuel Lechuga-Gerónimo), enid.partida@outlook.com (Enid Partida-Herrera).

Historial del manuscrito: recibido el 30/06/2024, ultima versión-revisada recibida el 18/10/2024, aceptado el 16/10/2024, publicado el 30/11/2024. **DOI:** https://doi.org/10.29057/icbi.v12iEspecial4.13344

1. Introduction

Rockets are extremely complex and sophisticated systems, as well as extremely useful and unique in their kind. They allow the transport of useful loads that, without them, would not be possible to use.

The clearest example is satellites, whose popularity has increased dramatically in recent years thanks to the efforts of companies such as *Orbex*, *PLD Space* and *SpaceX*, which have managed to get the international space community to place a satellite into orbit (Gallego Sanmiguel, 2020); especially those of the CubeSat type: a class of compact and modular satellites with cubic geometry.

When it comes to missions as important as putting a satellite into orbit, no component or detail is insignificant, where the highest priority is the successful completion of the mission. In the field of rockets, this is only possible thanks to the thrusters, a fundamental part of this study. A mission refers to a scientific endeavor that involves the use of payload to carry out various tasks, such satellite's deployment.

Thrusters have been used since the mid-20th century and have since become an irreplaceable part of rockets: they are incredibly powerful and capable of moving large payloads in the order of tons of mass. However, they are far from perfect, as they have vulnerabilities like other space actuators. Probably, the biggest area of opportunity is the lack of redundancy in the event of a fatal failure of one, since a rocket has a large number.

Certainly, thruster failure can come from many sources. For example, the nozzle, gaskets, Electronic Control Unit, thruster release valve, etc (Haught and Duncan, 2014). However, the most prone part, because it has movement, is the attitude control actuator. The current study will focus on this part.

This article presents five main sections, listed as follows.

1. Notation, for the mathematical symbols used.
2. State of art, to study the main types of attitude control in rockets and define what can be done to improve.
3. Proposal, to propose a solution methodology as well as preliminary considerations.
4. Modeling, to present the mathematical and physical foundations that govern the proposal.
5. Conclusions, to comment on what has been addressed in this work and propose future and complementary work.

2. Notation and Acronyms

The notation and abbreviations used along this work are established as follows.

2.1. Notation

- **A**: Matrix.
- $\boldsymbol{a}$: Vector.
- $\hat{\boldsymbol{a}}$: Unitary vector.
- a: Scalar.

2.2. Acronyms

- BFF: Body-Fixed Frame.
- ECI: Earth-Centered Inertial frame.
- RW: Reaction Wheel.
- RWA: Reaction Wheel Array.
- RRWA: Reconfigurable Reaction Wheel Array.
- TVC: Thrust Vector Control.

3. State of the art in rocket attitude control

The state of the art in rockets is extensive and well documented, which is motivated by the creation of start-ups that are dedicated to the manufacture of rockets either for the launch of satellites or satellite networks. As an example, the company Orbex Space is developing its first rocket called *Orbex Prime*, which has a unique ecological propellant and consists of two stages plus a payload (Orbital-Express-Ltd, 2018), as exemplified in figure 1.

3.1. Reference Frames

In the rocket's field, there are two main frames of reference.

1. **Body-Fixed Frame (BFF)**.
   This frame is denoted by the subscript b, the origin of which is at the center of mass of the rocket, represented by the point with symbol o_b. The axis $\hat{\boldsymbol{x}}_b$ is deployed towards the tip of the rocket, while $\hat{\boldsymbol{y}}_b$ is deployed perpendicularly towards the side of the rocket. The axis $\hat{\boldsymbol{z}}_b$, on the other hand, completes the right-hand rule. (Chessab Mahdi, 2018).
   For the purposes of this study and, at the same time, to emphasize it's rocket's, the frame will be identified with the subscript r. An illustration is given in figure 1.
2. **Earth-Centered Inertial frame (ECI)**.
   This frame of reference is extremely useful for describing the trajectory of the rocket in orbit. It is denoted by the subscript i and finds its origin at the center of the earth, marked by a point o_i. Unlike the previous frame, this one does not rotate with the reference object; that is, the Earth, so it is fixed in space.
   The $\hat{\boldsymbol{z}}_i$ axis points toward the geographic north pole, while the $\hat{\boldsymbol{x}}_i$ axis points to the summer equinox of the northern hemisphere. Finally, the axis $\hat{\boldsymbol{y}}_i$ completes the orthogonal system according to the right-hand rule (Lechuga-Gerónimo, 2023)

It also happens that, in the literature, it is common to observe that the angles produced by the inclination receive a particular name for each axis. For $\hat{\boldsymbol{x}}$, $\hat{\boldsymbol{y}}$ and $\hat{\boldsymbol{z}}$ are called *roll*, *pitch* and *yaw*; respectively (Sidi, 1997).

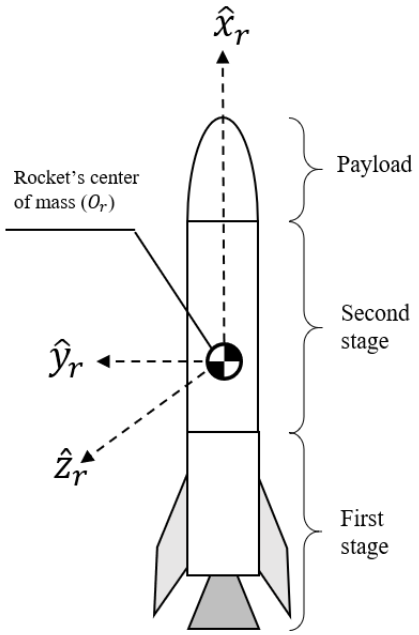

Figure 1: Rocket's stages and main axes.

In next subsection, a brief description of control types for rockets is offered as a manner of context for the following sections.

3.2. Control Types

Rockets have different control types, based on actuators, to modify attitude during launch. The main types are mentioned below.

1. **Vernier thrusters.**
   They were once the main method of modifying the thrust vector. Currently, they have been replaced by other methods on this list.
   These devices are small thrusters located on one side of the main thrusters or on the side of the rocket body, and activated when required. Unlike others, these are static type, which means that they are not equipped with movement (Hall, 2023).
   Despite having been the favorite of engineers at the beginning of rockets, today, Vernier thrusters are out of use because simpler and more efficient ways have been found to modify the thrust vector.
   An illustration of this type of control is given in part c) of figure 2.
2. **Movable Fins.**
   As their name indicates, they are a group of fins located on the sides of the rocket body. Its purpose is to rotate with respect to a frame of reference congruent with the body, and thereby offer a change in the direction of thrust (Hall, 2023).
   This type of control is illustrated in part a) of figure 2.
3. **Thrust Vector Control (TVC).**
   The Thrust Vector Control (TVC) actuators are the most common type and currently used in diverse systems, such in Orbex Prime rocket (Orbital-Express-Ltd, 2018), to modify the direction of thruster's thrust in order to control the attitude (Crown and Weir, 1993).
   They consist of two motors that move or rotate a mechanism equipped with a lever connected by a joint to the body of the nozzle. When the actuator is activated, they modify the orientation of the rocket, which ultimately manipulates the attitude vector of the rocket. The other end of the actuator remains anchored to the rocket body at all times (Li et al., 2012).
   The movement of the nozzle is possible thanks to the gimbal joint, which allows it to rotate in the axes $\hat{\boldsymbol{x}}_r$ and $\hat{\boldsymbol{y}}_r$ simultaneously and independently.
   The use of a gimbal joint was a reason for the exclusion of this type of actuator for a long time, since the designers did not trust that the gaskets were useful enough not to leak propellant. A very similar situation happened with the hoses, since they had to be flexible for the application. Also, this type of control was not able to be implemented satisfactorily until there was sufficient confidence in the operation of the servomotors or valves, depending on the type of actuation. Gas-actuated pistons are sometimes chosen instead of electric motors as actuators (Sopegno et al., 2023).
   An image of the TVC control type is presented in part b) of figure 2.
   On the other hand, in figure 3, a detailed illustration of the TVC control type and its components is offered on a BFF type reference frame and congruent with that of the nozzle body, distinguished by the subscript n.
4. **Thrust Vane.**
   This method is perhaps the oldest of all. It is based on placing a movable vane inside the nozzle, which when moved, modifies the direction of the flow and with it, the attitude of the rocket (Hall, 2023).
   A representation of this type of control is given in part d) of figure 2.

Once the different types of rocket attitude control have been established, it is clear that Reaction Wheels (RW) are not mentioned. This is a very important topic, which is discussed in the next section.

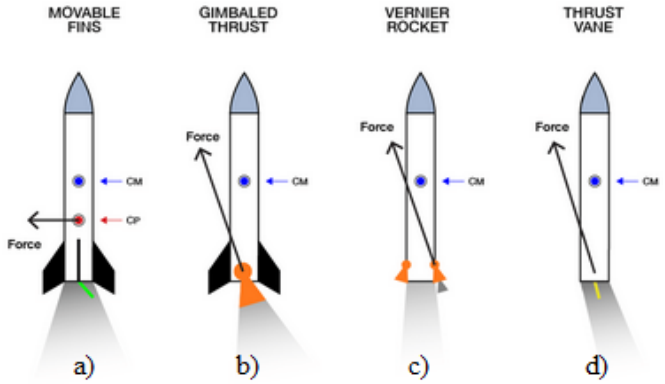

Figure 2: Control types for rockets. a) movable fins, b) gimbaled thrust, c) vernier rocket, d) thrust vane. (Li et al., 2012).

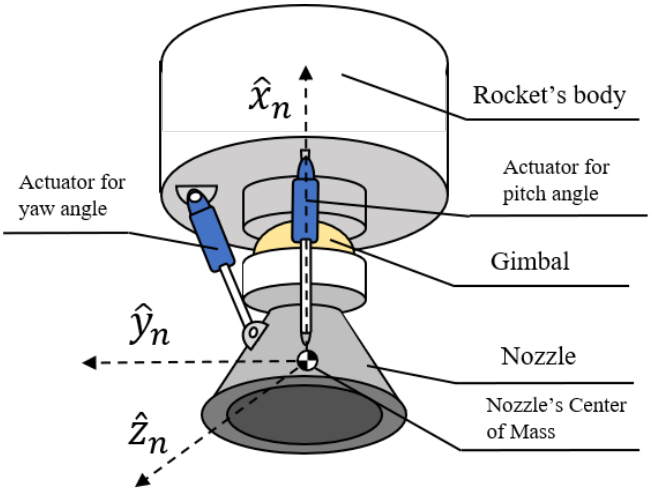

Figure 3: TVC lay-out for one-single nozzle.

3.3. Reaction wheels as a type of attitude control

Reaction wheels have been widely and successfully used for attitude control of aerospace objects of all kinds: aircraft, drones, and even the Hubble telescope and the International Space Station; but mainly, satellites (Shirazi and Mirshams, 2014). It is rather strange that such a versatile active actuator does not appear in any control type, as RW is a fundamental and essential part of attitude control (Lechuga-Geronimo, 2017).

Figure 4 presents a simplified illustration of a reaction wheel within a BFF-type frame, denoted by the subscript a, originating from its center of mass and pointing towards the $\hat{\boldsymbol{y}}_a$ axis. The frame a will be used later to refer to a specific actuator.

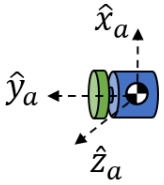

Figure 4: Reaction Wheel in a BFF congruent with the actuator. In blue, the motor. In green, the inertia disk.

Typically, reaction wheels are located aligned with the center of mass of the inertial body, making the generated torque more effective (Sugita, 2017). However, in rockets this cannot be possible, as explained below.

Although reaction wheels are actuators with remarkable qualities, such as a high level of precision and efficiency (Lechuga-Gerónimo et al., 2021), they are not applicable to rockets due to their enormous amount of mass, which is usually in the order of tons (Orbital-Express-Ltd, 2018). This makes reaction wheels not viable because they would require colossal mass and dimensions to generate sufficient angular momentum for such a purpose.

However, there is the possibility of using reaction wheels for rocket attitude control effectively under a TVC-based approach. If the conventional electromechanical actuators of the TVC were replaced, and reaction wheels were placed in their place, the nozzle could rotate instead of the rocket body, and therefore, achieving a change in attitude. This idea, although it may seem daring, has a first support that consists in the fact that the nozzle has a mass many times smaller than that of the rocket, so it is assumed that the RW could have adequate physical properties.

Even if one of the wheels fails, there are methods to increase its redundancy. In a recent study, available in (Lechuga-Gerónimo, 2023), a novel approach was presented in which a method for attitude control is designed that consists of relocating the reaction wheels inside the body of a CubeSat-type satellite in order to increase the maximum angular momentum capacity or replace one that entered fatal failure mode; in which case it is difficult to continue with the mission.

If the above application is extrapolated to rocket attitude control, it could be useful as an alternative to TVC actuators.

These ideas and conjectures lead to the development of the proposal in the following section. However, it is first necessary to present the Reaction Wheel Array (RWA).

3.4. Reaction Wheel Array

As described above, reaction wheels have improved properties when placed in arrays (Ismail and Varatharajoo, 2010). For example, increased redundancy in case of failure and increased ability to generate angular momentum as well.

There are a variety of RWAs available in the state of the art, but the ones that are applied to rockets are mainly two (Sidi, 1997); which are detailed below.

- Two RW in Parallel (2-P).
  This array has two reaction wheels coincident with two axes of the reference frame to which they are aligned; usually, the body to be rotated. The axes can be any combination of two vectors. This RWA offers partial attitude control.
  An illustration of the 2-P array is given in a) of figure 5.

- Three RWs in Orthogonal (3-O).
  Similar to the above, where there are three reaction wheels located on each axis of the reference frame. This RWA offers full attitude control, as it has one principal axis actuator.
  An illustration of 3-O array can be seen in b) of figure 5.

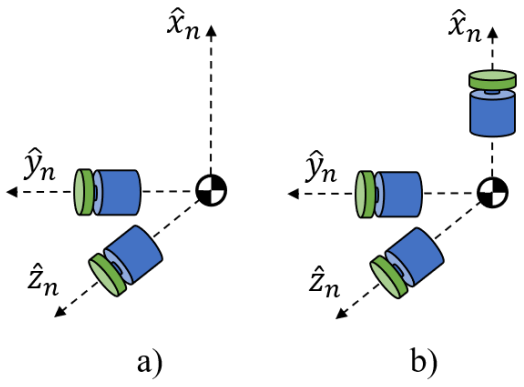

Figure 5: Two Reaction Wheel Arrays (RWA): a) 2-P, b) 3-O.

4. Proposal for using reaction wheels as actuators for a type of control based on TVC

In the previous sections, it was explained that the idea of using reaction wheels is appropriate as long as they are used to modify the attitude of the nozzle, and not directly of the rocket body.

In contrast, in this section the development of this hypothesis is presented, establishing some preliminary considerations, with the intention that its mathematical modeling be carried out in the following section.

The first thing to consider are the reference frames, which are three: a, n and r; the first at the level of the actuator, the second when it refers to the nozzle, and the third to the rocket itself.

However, the attitude of the rocket, distinguished by the frame r, is not of direct interest for this study because the central idea lies in the use of RWs for the control of the nozzle attitude. This means that the frame r will be considered fixed in space, so it will be anchored to a null attitude. This will allow a better observation of the changes in the nozzle attitude. Thus, for example, when the nozzle frame attitude n is zero, it will be coincident with r as illustrated in figure 6, and as expressed in equation (1).

$$\begin{bmatrix}\phi_n & \theta_n & \psi_n\end{bmatrix} = \begin{bmatrix}\phi_r & \theta_r & \psi_r\end{bmatrix} = \begin{bmatrix}0 & 0 & 0\end{bmatrix} \tag{1}$$

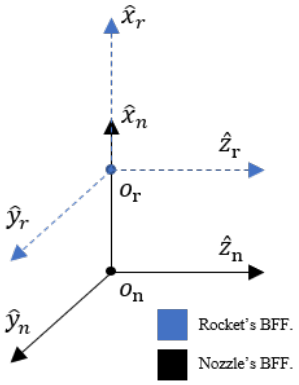

Figure 6: Rocket's and nozzle's reference frames when nozzle's attitude is null.

The next point to explain is about the nozzle's degrees of freedom, the number of which directly depends on the number of axes to be controlled. Under the assumption that only θ_n and ψ_n will be modified, then the number is two; which would provide partial attitude control. If, on the other hand, the rocket were subject to a rotation about $\hat{\boldsymbol{x}}_r$, then the number would be three, granting full attitude control.

The last topic before starting with the modeling is the Reconfigurable Reaction Wheel Array (RRWA). Its importance in mission survivability, increased redundancy, and other positive properties were explained, whose operation is summarized in the ability to relocate RWs within a RWA so that they acquire different orientation vectors.

Due to the large number of mathematical elements, the solution for this topic is developed in the next section.

5. System Modeling

The dynamic model of the nozzle is given by the Equations of Motion for rigid bodies, in the same way as it happens with satellites, rockets, drones, airplanes and others. This mathematical expression, in matrix form, can be seen in the equation (2).

$$\mathbf{I}_n\dot{\boldsymbol{\omega}}_n(t) + \boldsymbol{\omega}_n(t) \times (\mathbf{I}_n\boldsymbol{\omega}_n(t)) = \boldsymbol{\tau}_n(t) \tag{2}$$

Where $\mathbf{I}_n \in \mathbb{R}^{3\times3}$ is the inertia tensor of the nozzle, considered as a constant. $\boldsymbol{\omega}_n(t) \in \mathbb{R}^{3\times1}$ and $\dot{\boldsymbol{\omega}}_n(t) \in \mathbb{R}^{3\ times1}$ correspond to the angular velocity vectors of the nozzle and its numerical derivative, respectively. Finally, $\boldsymbol{\tau}_n(t) \in \mathbb{R}^{3\times1}$ is the vector of incident torques on the nozzle, with equivalent expression in the equation (3).

$$\boldsymbol{\tau}_n(t) = \boldsymbol{\tau}_a(t) + \boldsymbol{\tau}_d(t) \tag{3}$$

Where $\boldsymbol{\tau}_a(t) \in \mathbb{R}^{3\times1}$ and $\boldsymbol{\tau}_d(t) \in \mathbb{R}^{3\times1}$ are the torque vectors generated by the actuators and the environmental disturbances impinging on the nozzle, respectively.

After substituting the equation (3) into the equation (2), the equation (4) is obtained.

$$\mathbf{I}_n\dot{\boldsymbol{\omega}}_n(t) + \boldsymbol{\omega}_n(t) \times (\mathbf{I}_n\boldsymbol{\omega}_n(t)) = \boldsymbol{\tau}_a(t) + \boldsymbol{\tau}_d(t) \tag{4}$$

Reviewing the model given by equation (4), it is evident that the input of the system is the torque vector of the actuators, $\boldsymbol{\tau}_a(t)$, while $\dot{\boldsymbol{\omega}}_n(t)$ is the output. In order to generate an expression consistent with such input and output, it is suggested to restructure equation (4) and convert it into equation (5), and in turn, into equation (6).

$$\mathbf{I}_n\dot{\boldsymbol{\omega}}_n(t) = \boldsymbol{\tau}_a(t) + \boldsymbol{\tau}_d(t) - \boldsymbol{\omega}_n(t) \times (\mathbf{I}_n\boldsymbol{\omega}_n(t)) \tag{5}$$

$$\dot{\boldsymbol{\omega}}_n(t) = \mathbf{I}_n^{-1}[\boldsymbol{\tau}_a(t) + \boldsymbol{\tau}_d(t) - \boldsymbol{\omega}_n(t) \times (\mathbf{I}_n\boldsymbol{\omega}_n(t))] \tag{6}$$

Where it remains to numerically integrate $\dot{\boldsymbol{\omega}}_n(t)$, without forgetting the initial conditions $\boldsymbol{\omega}_n(0)$, to obtain $\boldsymbol{\omega}_n(t)$, as expressed in the equation (7).

$$\boldsymbol{\omega}_n(t) = \mathbf{I}_n^{-1}\int [\boldsymbol{\tau}_a(t) + \boldsymbol{\tau}_d(t) - \boldsymbol{\omega}_n(t) \times (\mathbf{I}_n\boldsymbol{\omega}_n(t))]dt \tag{7}$$

The remainder of the nozzle modeling is centered on two other parts: 1) the generation of torque $\boldsymbol{\tau}_a(t)$ by the reaction wheels and, 2) the representation of the attitude produced by the angular velocities $\boldsymbol{\omega}_n(t)$. Both points are developed in the following subsections.

5.1. Modeling of torque generation and transmission from the reaction wheels to the nozzle.

The equation (8) governs the generation of angular momentum from the reaction wheels (Daw-Kwan, 2014).

$$\boldsymbol{\tau}_a(t) = \dot{\mathbf{H}}_a(t) \tag{8}$$

where $\mathbf{H}_a(t) \in \mathbb{R}^{3\times1}$ is the angular momentum vector of the RW, which in turn is equivalent to the equation (9).

$$\mathbf{H}_a(t) = \mathbf{I}_a\boldsymbol{\omega}_a(t) \tag{9}$$

Here $\mathbf{I}_a \in \mathbb{R}^{3\times3}$ is the rotor inertia tensor. However, due to the physical limitation of the rotor that it can only rotate around

the vector it is located on, the inertia tensor $\mathbf{I}_a$ must be rewritten as a scalar, I_a, taking on only the value of the rotor moment of inertia and the rotor load, which is reflected in the equation (10).

$$\mathbf{H}_a(t) = I_a \boldsymbol{\omega}_a(t) \tag{10}$$

Combining equations (8) and (9) gives equation (11). The last expression establishes the origin of the angular momentum.

$$\boldsymbol{\tau}_a(t) = I_a \dot{\boldsymbol{\omega}}_a(t) \tag{11}$$

On the other hand, the transmission of angular momentum from the RW to the nozzle is given by the Principle of Conservation of Angular Momentum (PCAM), which establishes that the sum of all angular moments is equal to zero, which is illustrated in the equation (12), and is equivalent to what is expressed in the equation (13).

$$\mathbf{H}_a(t) + \mathbf{H}_n(t) = 0 \tag{12}$$

$$\mathbf{H}_a(t) = -\mathbf{H}_n(t) \tag{13}$$

This means that the angular momentum generated by a RW will cause angular momentum, torque and rotation in the nozzle in opposite directions.

By substituting the equation (10) into (13), gives the equation (14).

$$I_a \boldsymbol{\omega}_a(t) = -\mathbf{I}_n \boldsymbol{\omega}_n(t) \tag{14}$$

Since the momentum is generated by $\boldsymbol{\omega}_a(t)$ and transferred to $\boldsymbol{\omega}_n(t)$, a more appropriate expression is given in equation (15).

$$\boldsymbol{\omega}_n(t) = -\mathbf{I}_n^{-1}(I_a \boldsymbol{\omega}_a(t)) \tag{15}$$

This concludes the first point regarding system modeling. The next subsection discusses how to represent the nozzle attitude.

5.2. *Nozzle attitude representation method*

In order to determine the nozzle attitude, it is necessary to apply a conversion between angular rates and an attitude representation method. Quaternions are by far the preferred method to describe the attitude due to their efficiency, robustness and effectiveness. However, the variables of interest are the nozzle angles: $\phi_n(t)$, $\theta_n(t)$ and $\psi_n(t)$.

Given this case, there is a way to use both methods, and it consists of using quaternions as the internal attitude calculation algorithm and, on the other hand, converting them to Euler angles for better interpretation by the user.

The equation (16) describes the conversion between angular rates to quaternions.

$$\dot{\mathbf{q}}(t) = \frac{1}{2}\mathbf{W}(\mathbf{q})^T \boldsymbol{\omega}_n(t) \tag{16}$$

where $\mathbf{W}(\mathbf{q}) \in \mathbb{R}^{3\times4}$ is the quaternion shift matrix, and is given by the equation (17).

$$\mathbf{W}(\mathbf{q}) = \begin{bmatrix} -q_1 & q_0 & -q_3 & q_2 \\ -q_2 & q_3 & q_0 & -q_1 \\ -q_3 & -q_2 & q_1 & q_0 \end{bmatrix} \tag{17}$$

With the above, it only remains to apply the numerical integral of $\dot{\mathbf{q}}(t)$, as expressed in the equation (18), together with its initial attitude conditions $\mathbf{q}(0)$.

$$\mathbf{q}(t) = \frac{1}{2}\int \mathbf{W}(\mathbf{q})^T \boldsymbol{\omega}_n(t) \tag{18}$$

Once the attitude is obtained by this representation method, it can be converted to any other, such as the Euler angles already mentioned.

5.3. *Reconfigurable Reaction Wheel Array Modeling.*

The RRWA was recently introduced in a previous work, available in (Lechuga-Gerónimo, 2023), where the objective was to relocate the RWs in a trajectory defined by a topologically modified Möbius strip to coincide with the main axes of a body; now, a nozzle, but back then, a 3U CubeSat satellite. By this way, in case a RW fails, it can be replaced in the same vector by another RW at rest, thus ensuring the continuity of the mission.

The original Möbius strip is illustrated in figure 7, with its own reference frame M and the corresponding axes $\hat{\boldsymbol{x}}_{\boldsymbol{M}}$, $\hat{\boldsymbol{y}}_{\boldsymbol{M}}$ and $\hat{\boldsymbol{z}}_{\boldsymbol{M}}$. After several topological modifications extensively described in (Lechuga-Gerónimo, 2023), the product of figure 7 becomes the modified Möbius strip (hereafter Möbius–Lechuga strip), available in figure 8.

This last surface, the Möbius-Lechuga strip, has some improved properties. Its reference frame coincide fully with the satellite's axes, making it possible for a reaction wheel located at a starting point (i.e., *Point* $\hat{y}$), to move on the Möbius-Lechuga strip and reach all the coincident points *Point* $\hat{x}$, *Point* $\hat{y}$ and *Point* $\hat{z}$; and therefore, produce an angular momentum aligned with the $\hat{\boldsymbol{x}}_{\boldsymbol{M}}$, $\hat{\boldsymbol{y}}_{\boldsymbol{M}}$ and $\hat{\boldsymbol{z}}_{\boldsymbol{M}}$ of the Möbius-Lechuga strip and the satellite at the same time.

Furthermore, with these changes, it is possible to obtain combinations of vector components for the three axes. These vectors are denoted by $\boldsymbol{N}_{\hat{\beta}_1}$ and $\boldsymbol{N}_{\hat{\beta}_2}$. This work will focus on figure 8.

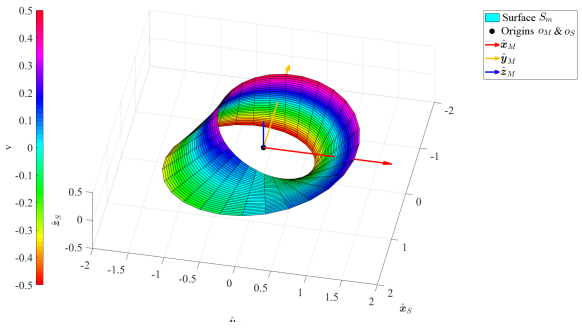

Figure 7: Original Möbius Strip (Lechuga-Gerónimo, 2023).

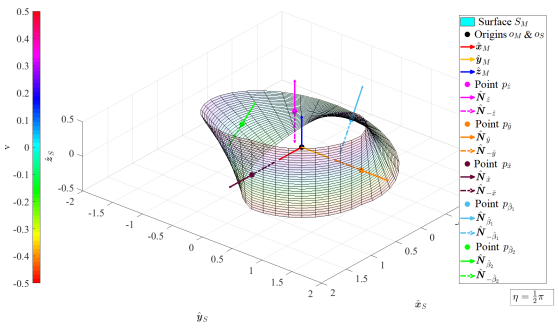

Figure 8: Möbius-Lechuga Strip (Lechuga-Gerónimo, 2023).

The structure of the Möbius-Lechuga strip is given by two surfaces: a circular one, C; and a twisted one, M, from which the normal vectors, $\hat{N}_C(u)$ and $\hat{N}_M(u)$, are obtained. The process of obtaining them is widely described in (Lechuga-Gerónimo, 2023), but it is not included in this work due to its length.

The vector components of the normal vectors, converted to coordinates of the nozzle frame n, are given by (19) and (20), where both equations describe the components of the normal vector as a function of the position along the Möbius-Lechuga strip given by u. The values for u are $u = [0 \leq u \leq 2\pi)$ since it corresponds to the circular and longitudinal position along the strip. Finally, x, y and z are the vector components.

Normally, when talking about a circular surface, the maximum value of u would be $u = 2\pi$. At this point, we return to the same place on the surface with exactly the same normal vector components. However, since this is a recursive surface, going from $u = 2\pi$ we return to the starting point but in the opposite direction. It is only when $u = 4\pi$ that we obtain the same starting point and the same vectors as at the point $u = 0$.

$$\hat{\mathbf{N}}_C(u) \begin{cases} y_C(u) = \dfrac{-\sin(u)}{\sqrt{|\cos(u)|^2 + |\sin(u)|^2}} \\ z_C(u) = \dfrac{\cos(u)}{\sqrt{|\cos(u)|^2 + |\sin(u)|^2}} \\ x_C(u) = 0 \end{cases}, \quad \tfrac{3}{2}\pi \leq u < 2\pi \tag{19}$$

$$\hat{\mathbf{N}}_M(u) \begin{cases} y_M(u) = \dfrac{\cos\left(\frac{2}{3}u\right)\sin(u)}{\sqrt{|\sin\left(\frac{2}{3}u\right)|^2 + |\cos\left(\frac{2}{3}u\right)\cos(u)|^2 + |\cos\left(\frac{2}{3}u\right)\sin(u)|^2}} \\ z_M(u) = \dfrac{\cos(\frac{2}{3}u)\cos(u)}{\sqrt{|\sin\left(\frac{2}{3}u\right)|^2 + |\cos\left(\frac{2}{3}u\right)\cos(u)|^2 + |\cos\left(\frac{2}{3}u\right)\sin(u)|^2}} \\ x_M(u) = \dfrac{\sin(\frac{2}{3}u)}{\sqrt{|\sin\left(\frac{2}{3}u\right)|^2 + |\cos\left(\frac{2}{3}u\right)\cos(u)|^2 + |\cos\left(\frac{2}{3}u\right)\sin(u)|^2}} \end{cases}, \quad 0 \leq u < \tfrac{3}{2}\pi \tag{20}$$

It is then necessary to define a path function that depends on u capable of handling $0 \leq u \leq 2\pi$. That expression is available in the equation (21).

$$T(u) = \begin{cases} \hat{\mathbf{N}}_M(u), & \text{if} \quad 0 \leq u(t) < \frac{3}{2}\pi \\ -\hat{\mathbf{N}}_C(u), & \text{if} \quad \frac{3}{2}\pi \leq u(t) < 2\pi \\ -\hat{\mathbf{N}}_M(u), & \text{if} \quad 2\pi \leq u(t) < \frac{7}{2}\pi \\ \hat{\mathbf{N}}_C(u), & \text{if} \quad \frac{7}{2}\pi \leq u(t) < 4\pi \end{cases} \tag{21}$$

A representation of the culmination of this proposal is given in figure 9, where it is shown how one or more RWs of a RWA can move around a nozzle given a trajectory marked by the Möbius-Lechuga strip. Note also the points of interest for which $u(t)$ returns a coincidence with the vectors of the nozzle's reference frame. The normal vectors obtained based on the trajectory, in addition to indicating the orientation of wheels, directly influence the direction of generation of angular momentum, according to equation (22), as an alternative expression of equation (10), where the unit vector of the angular velocity of the RW, $\hat{\omega}(u) \in \mathbb{R}^{3\times1}$, depends directly on $u(t)$.

$$\boldsymbol{H}_a(t) = I_a\hat{\omega}_a(u)\omega_a(t) \tag{22}$$

Acknowledgements

The first author would like to express his gratitude to CINVESTAV-IPN and CONAHCyT for the financial support that enabled the development of this research project. He also thanks Dr. Wen Yu-Liu for his mentorship.

The second author would like to express her gratitude to CENAGAS and also to Dr. Erika Virginia De Lucio-Rodríguez for her mentoring.

Conclusions

In this work it was studied that reaction wheels, despite being extremely versatile, precise and robust actuators, did not have a role in rocket attitude control due to physical limitations in mass and volume. However, a suitable alternative was proposed by replacing the conventional electromechanical actuators of classic TVC type control method with reaction wheels.

This proposal, considered as the main contribution of the article, proposes what would allow an improvement in the redundancy and performance of the actuators for the rocket attitude; increasing the probability of successfully completing the mission for which it was designed, created and launched. One pending topic to work on is the disturbance's mitigation.

In addition, the use of a surface so little used in engineering as the Möbius Strip has provided an innovative and creative approach, especially for an aerospace application.

Although the detailed engineering and mechanical design proposal of this remains as future work, it is clear that it presents a precedent for importing technical solutions from one application to another, with special attention to the technological boom in space and rocket engineering.

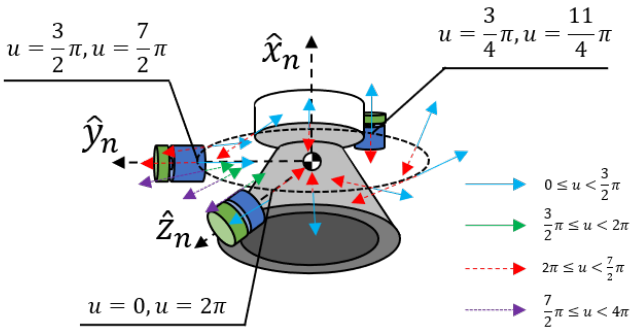

Figure 9: Trajectories of the normal vectors to the Möbius-Lechuga strip, according to $u(t)$.

References

Chessab Mahdi, M. (2018). *Attitude Stabilization for CubeSat: Concepts and Technology*. Cambridge Scholars Publishing, 1 edition. https://www.cambridgescholars.com/product/978-1-5275-0651-0.

Crown, J. and Weir, R. A. (1993). Design and test of electromechanical actuators for thrust vector control. Technical report, National Aeronautics and Space Administration. https://ntrs.nasa.gov/api/citations/19940025147/downloads/19940025147.pdf.

Daw-Kwan, K. (2014). Micro-vibration model and parameter estimation method of a reaction wheel assembly. *Journal of Sound and Vibration*, 333:4214–4231.

Gallego Sanmiguel, P. (2020). Miura 5: The european and reusable microlauncher for cubesats and small satellites. *Small Satellites Conference*, 34. https://digitalcommons.usu.edu/smallsat/2020/all2020/63/.

Hall, N. (2023). Rocket control. https://www1.grc.nasa.gov/beginners-guide-to-aeronautics/rocket-control/.

Haught, M. and Duncan, G. (2014). Modeling common cause failures of thrusters on iss visiting vehicles. *Probabilistic Safety Assessment and Management PSAM*. https://ntrs.nasa.gov/api/citations/20140004797/downloads/20140004797.pdf.

Ismail, Z. and Varatharajoo, R. (2010). A study of reaction wheel configurations for a 3-axis satellite attitude control. *Advances in Space Research*, 45:750–759. https://doi.org/10.1016/j.asr.2009.11.004.

Lechuga-Geronimo, V. M. (2017). Propuesta de control en cascada para la actitud de un satélite cubesat 1u. Technical report, Instituto Politécnico Nacional (IPN). http://dx.doi.org/10.13140/RG.2.2.25767.56486.

Lechuga-Gerónimo, V. M. (2023). Diseño de un arreglo reconfigurable de ruedas de reacción basado en la banda de möbius para el control de actitud de satélites cubesat. Master's thesis, Centro de Investigación y de Estudios Avanzados del Instituto Politécnico Nacional. http://dx.doi.org/10.13140/RG.2.2.26699.60963.

Lechuga-Gerónimo, V. M. et al. (2021). Cascade control for a 1u cubesat satellite. *Congreso Nacional de Ingeniería Electromecánica y de Sistemas (CNIES)*, 1(XX):486–490. https://www.researchgate.net/publication/357240551.

Li, Y., Lu, H., Tian, S., Yao, J., and Chen, J.-T. (2012). Posture control of electromechanical-actuator-based thrust vector system for aircraft engine. *IEEE Transactions on Industrial Electronics - IEEE TRANS IND ELECTRON*, 59:3561–3571.

Orbital-Express-Ltd (2018). Azul- azores micro launcher deimos and orbex. Technical report, Deimos Elecnor Group. https://esamultimedia.esa.int/docs/space_transportation/AZUL-ESA_Workshop-Export.pdf.

Shirazi, A. and Mirshams, M. (2014). Pyramidal reaction wheel arrangement optimization of satellite attitude control subsystem for minimizing power consumption. *International Journal of Aeronautical and Space Sciences*, 15:190–198. https://doi.org/10.5139/IJASS.2014.15.2.190.

Sidi, M. J. (1997). *Spacraft Dynamics and Control: A Practical Engineering Approach*. Cambridge University Press, 1 edition. https://doi.org/10.1017/CBO9780511815652.008.

Sopegno, L., Livreri, P., Stefanovic, M., and Valavanis, K. P. (2023). Thrust vector controller comparison for a finless rocket. *Machines*, 11(3). https://www.mdpi.com/2075-1702/11/3/394.

Sugita, M. (2017). Torque distribution algorithm for effective use of reaction wheel torques and angular momentums. *Acta Astronautica*, 139:18–23. https://doi.org/10.1016/j.actaastro.2017.06.014.